Supporting Information

Highly sensitive and uniform surface-enhanced Raman spectroscopy from grating-integrated plasmonic nanograss

Yang Shen, Xizhe Cheng, Guozhen Li, Qiangzhong Zhu, Zhenguo Chi, Jianfang Wang*, Chongjun Jin*

* E-mail: jinchjun@mail.sysu.edu.cn, jfwang@phy.cuhk.edu.hk

S1. Details on GIGNs fabrication.

Interference Lithography: The fabrication procedure is schematically shown in Fig. 1a. A 50-nm PMMA (molecular weight: 350,000, 1.5 wt% in chlorobenzene) film was first spin-coated on a cleaned quartz slide at 4000 rpm for 35 s, which functions as an adherent to ensure the firm attachment of the photoresist grating. The PMMA film was then treated on a hot plate at 180 ^{o}C for 5 min to evaporate chlorobenzene. A positive photoresist (AR-P 3740, Allresist) film was then spun onto the PMMA film, followed by a bake at 95 ^{o}C for 2 min. Its thickness was tuned from 125 to 225 nm by spin speed. The photoresist film was thereafter subjected to an exposure under an interference pattern of two continuous laser beams (457.9 nm). The incidence angles of the two laser beams on the photoresist film were 40.7^{o}, 34.8^{o}, 30.5^{o} and 22.4^{o}, determining the lattice constants of the grating of 350, 400, 450 and 600 nm, respectively. After the exposure, the photoresist film was immersed in a developer (AR 300-26, Allresist) at 21 ^{o}C for 12 s to give a photoresist grating.

PDMS molding: A molding using h-PDMS/s-PDMS composite was employed. Before PDMS molding, the master was placed in a vacuum desiccator, together with a Petri dish containing a few drops of Tridecafluoro-1,1,2,2-tetrahydrooctyl-1-trichlorosilane (TFOCS, Sigma-Aldrich) for 30 min. This process ensured that the entire surface of the photoresist grating was covered by a monolayer of TFOCS molecules through siloxane bonding, which prevents the cured PDMS from sticking to the master. To prepare h-PDMS, a mixture of 3.4 g of (7-8% vinylmethylsiloxane)-(dimethylsiloxane) copolymer (VDT-731, Gelest), 100 mg of 1,3,5,7-tetramethylcyclotetrasiloxane (SIT7900.0, Gelest) and 50 mg of platinum divinyltetramethyldisiloxane (SIP6831.1, Gelest) was stirred and degassed for 5 min. 1 g of (25-30% methylhydrosiloxane)-(dimethylsiloxane) copolymer (HMS-301, Gelest) was then added into this mixture and quickly stirred. Immediately (within 3 min), a thin layer of h-PDMS film was spin-coated onto a TFOCS-modified master at 1000 rpm for 35 s and cured for 20 min at 70 °C. A liquid-state mixture of 30 g of the base and 3 g of the curing agent (Sylgard 184, Dow Corning) was poured onto the h-PDMS layer and cured at 70 °C for 5 h to generate an h-PDMS/s-PDMS composite. Finally, peeled from the surface of the master, an h-PDMS/s-PDMS substrate with periodic grooves was obtained.

Metal deposition: A glancing electron beam evaporation of 5-nm nickel and 120-nm gold (the angle between the direction of deposition and the normal of the sample surface is ~80^{o}) along the

direction of the grooves was applied to form the oriented gold nanorods arrays on the groove-embedded PDMS substrate, namely GIGN.

S2. Details on adsorptions of probe molecules.

For R6G and MGITC detections, a drop of 10 μl of R6G (Sigma-Aldrich) or MGITC (Invitrogen) dissolved in deionized water was first added onto the surface of GIGN. After 1 h, the functionalized GIGN was washed with deionized water to remove excess molecules that were not bound to the metal surface, and then dried by flowing nitrogen. For adenine and cytosine detections, an oxygen plasma etching for 15 s was applied in advance to render the surface of GIGN hydrophilic. 2 μl of adenine (Sigma-Aldrich) or cytosine (Sigma-Aldrich) aqueous solution was then dripped onto the surface of GIGN and dried naturally in a clean bench.

S3. Details on SERS measurements.

All SERS spectra were performed on a Raman spectrometer (LabRAM HR, HORIBA Scientific). The p-polarized 633 nm laser with the power of 0.06 mW on the film was applied. An Objective lens (NA=0.9, 100×) was used to focus the laser beam on the samples (spot size is ~2 μm in diameter) and collect the backscattered Raman signals. The signal acquisition time of R6G, MGITC, adenine and cytosine were 10, 20, 40 and 40 s, respectively. For height- and periodicity-resolved SERS spectra, five measurements were made to determine the standard deviations of the Raman intensity for each sample. For the measurements of concentration-dependent SERS spectra, the multiple GIGNs with nearly identical geometry were prepared from the same sample, with each GIGN for one concentration. For Raman mapping, the point by point scanning mode with step size of 10 μm was carried out in an area of 80×80 μm^2 and the measurement configuration at each collection point was identical to the single measurement.

S4. FDTD simulations.

The simulations were performed using a commercial software (FDTD solutions, Lumerical Solutions) to generate the absorption spectra and electric field distributions of the involved structures in this paper. The structure was excited with p-polarized plane-wave light. Bloch boundary conditions were applied in both *x*- and *y*-axes. A mesh size of 3 nm for the metal region was utilized. The dielectric permittivity of gold is taken from Johnson and Christy. The used refractive indices for the h-PDMS and s-PDMS were both 1.4. In addition, to simulate a randomly arranged nanorods assembly, a random location deviation of 50% was applied in *x*- and *y*-axes.

S5. Top-view and cross-sectional SEM images of the gold nanograss fabricated on the flat quartz substrate for determining the sizes of gold nanorods

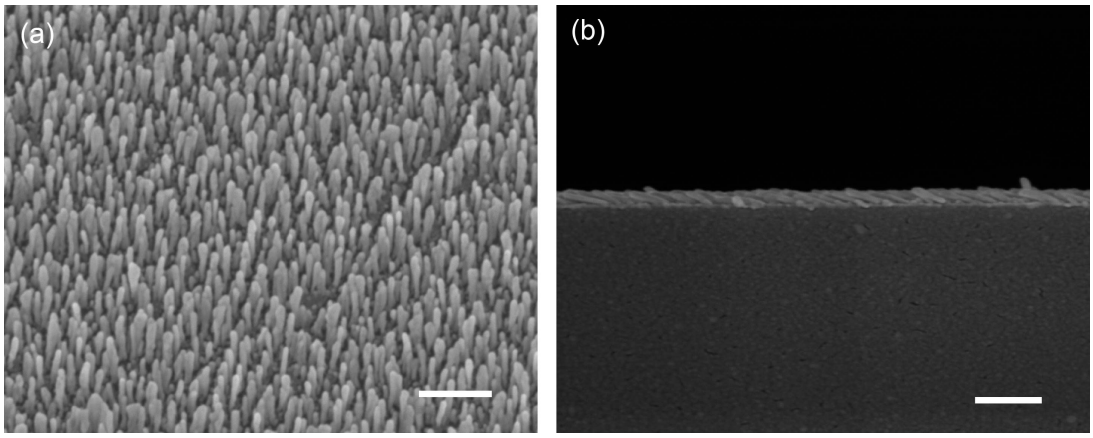

Fig. S1. SEM images of a typical gold nanograss on the flat quartz substrate. (a) top-view SEM image; (b) cross-sectional SEM image. The sizes of gold nanorods are $l = 120 \pm 15$nm, $d = 25 \pm 5$ nm, $\theta = 15^{o}$, $s_x = 37$ nm and $s_y = 80$ nm. Scale bars, 2 μm.

S6. Simulations showing the far-field and near-field optical properties of the uniform and random GIGNs

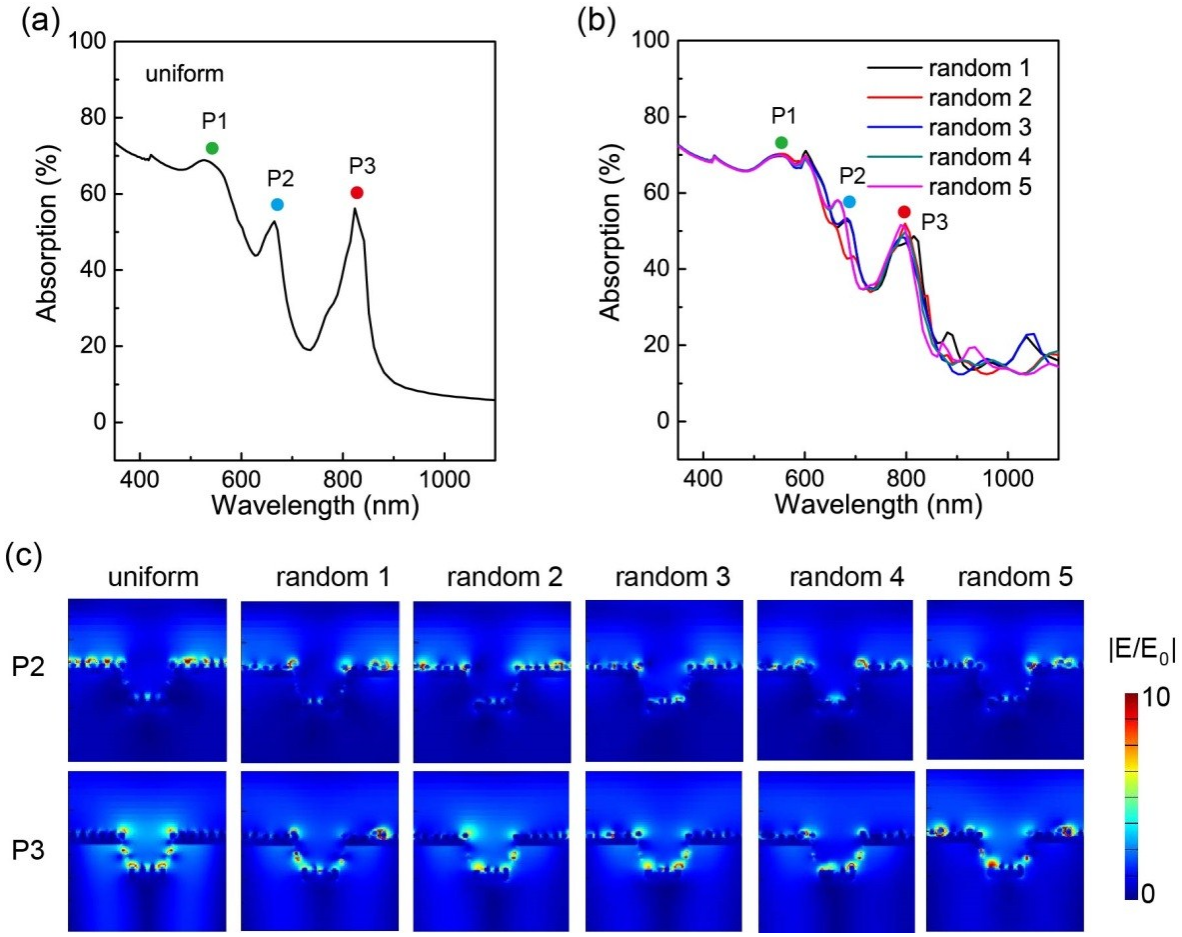

Fig. S2. Comparison of the simulated far-field and near-field optical properties of the two

structures, where gold nanorods are uniformly and randomly arranged on the dielectric grating respectively. (a) Simulated absorption spectrum of a uniformly arranged nanorods assembly. (b) Simulated absorption spectra of five randomly arranged nanorods assemblies with a random location deviation of 50% applied in both *x*- and *y*-axes. It is found that the random ones also exhibit three peaks at the nearly same wavelength positions as the uniform one. (c) Simulated electric field distributions of the uniform and random gold nanorods assemblies at P2 and P3 peaks, respectively, at the linear scale. Similarly, the hotspots caused by in-plane diffractions also exist even in random nanorods on the dielectric grating. The sizes of the grating-integrated nanorods assembly are a = 600 nm, h = 150 nm, w_1 = 400 nm, w_2 = 470 nm, l = 120 nm, d = 25 nm, θ = 15°, s_x = 37 nm and s_y = 80 nm.

S7. Simulations showing the origins of P2 and P3 modes

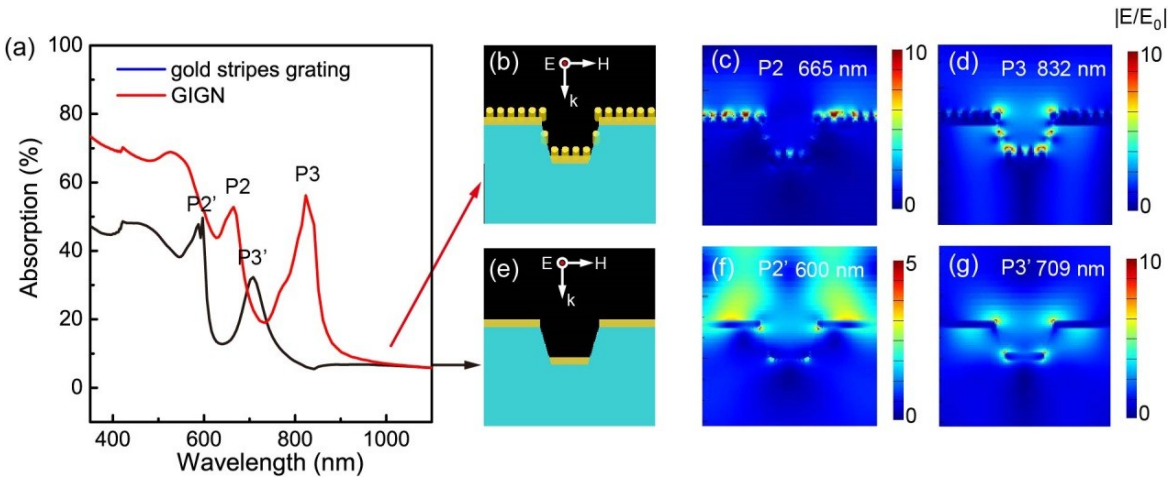

Fig. S3. P2 and P3 are originated from the strong coupling between LSPRs of individual gold nanorods assemblies and Wood's anomalies in air and PDMS grating, respectively. (a) Absorption spectra of a GIGN (red curve) and a structure containing only the gold stripes grating but without the nanorods (black curve), respectively. (b-d) Schematic and simulated electric field intensity distributions of the GIGN at P2 and P3 peaks, respectively, at the linear scale. (e-g) Schematic and simulated electric field intensity distributions of the gold stripes grating at P2' and P3' peaks, respectively, at the linear scale. The sizes of the GIGN and gold stripes grating are a= 600 nm, h= 150 nm, w_1= 400 nm, w_2= 470 nm, l= 120 nm, d= 25 nm, θ = 15°, s_x = 37 nm and s_y = 80 nm.

S8. Measured absorption spectrum and SERS spectra of a GIGN under 514 nm and 633 nm excitations

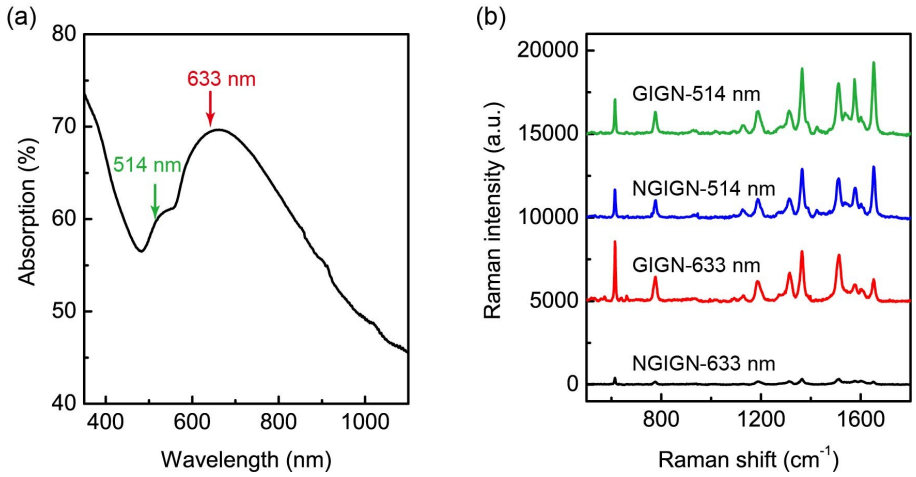

Fig.S4. Comparison of SERS performances under the excitations with 514 nm and 633 nm laser lines. (a) Absorption spectrum of a GIGN (a = 400 nm, h = 150 nm). Clearly, this GIGN couples with 633 nm laser line rather than 514 nm. (b) SERS spectra of GIGN (a = 400 nm, h = 150 nm) and NGIGN under the excitations using 514 and 633 nm laser sources. The powers of 514 nm and 633 nm lasers are 0.02 and 0.06 mW, respectively. The acquisition time are both 20 s. The SERS intensity of GIGN under 633 nm (nonresonant Raman) and 514 nm (resonant Raman) excitations are roughly same, however, I_{GIGN}/I_{NGIGN} for 633 nm laser line (~10) is much higher than that for 514 nm laser line (< 2). There is little effect on strengthening the SERS signals for GIGN under 514 nm excitation owing to the absence of strong plasmon resonance at this wavelength.

.

S9 The optimal height of groove revealed by the simulated height-dependent absorption spectra and electric field intensity distributions

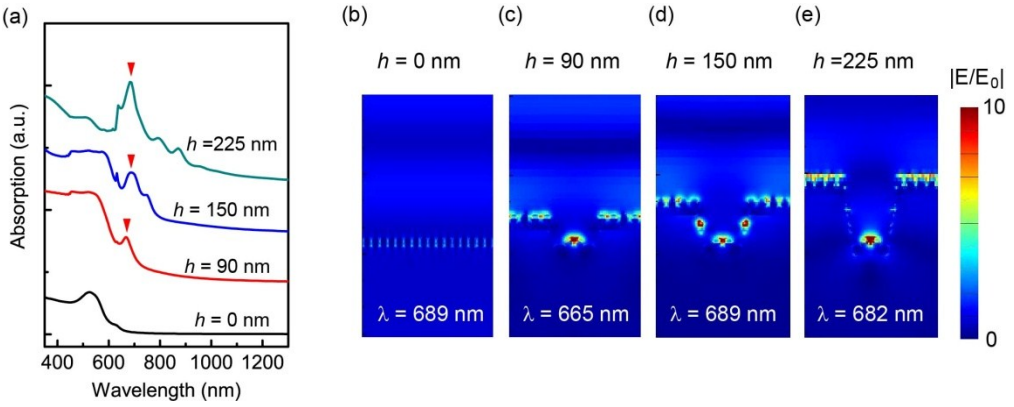

Fig. S5. Simulated absorption spectra and electric field intensity distributions of GIGNs with different groove heights from 0 to 225 nm. The sizes of the GIGN are a = 450 nm, l = 120 nm, d = 25 nm, θ= 15°, s_x = 37 nm and s_y = 80 nm. From the absorption spectra shown above, as h is increased from 0 to 225 nm, peak P3 (indicated by the red triangles, arising from the interaction between upper and lower gold nanorods assembly via diffraction in the periodic grooves) emerges and is gradually strengthened. Specifically, as h = 150 nm, the hot spots are localized at both the bottom and side walls of the groove, which seems to approach the optimal distributions.

Differently, the shallower groove is inclined to behavior as a nanorods assembly on a flat substrate, and the deeper groove begins to weaken the coupling between the top and bottom nanorods, which both hamper the hot spots generations in the side walls of the groove. On the other hand, for SERS spectra of R6G, the main intrinsic peaks (1200~1600 cm^{-1}) correspond to the Raman scattering light at the wavelength of 685 ~704 nm (for 633 nm excitation). For the GIGNs in experiment, as *h* is from 125 to 170 nm, the P3 of them couple with the Raman scattering light at this range, whereas P3 decouple with Raman scattering light as *h* = 225 nm. Hence, at the case of coupling to the Raman scattering light, the height of 150 nm is an apparently optimal parameter and produces highest efficiency. Note that the simulated absorption peak P2 (caused by the coupling between LSPR of the upper stripe of gold nanorods assemblies and Wood's anomalies in air) is missing, because this resonance is close to and finally merges into the LSPR of the nanorods.

S10. Intensity mapping of SERS signals of R6G molecules adsorbed on a GIGN at other Raman bands.

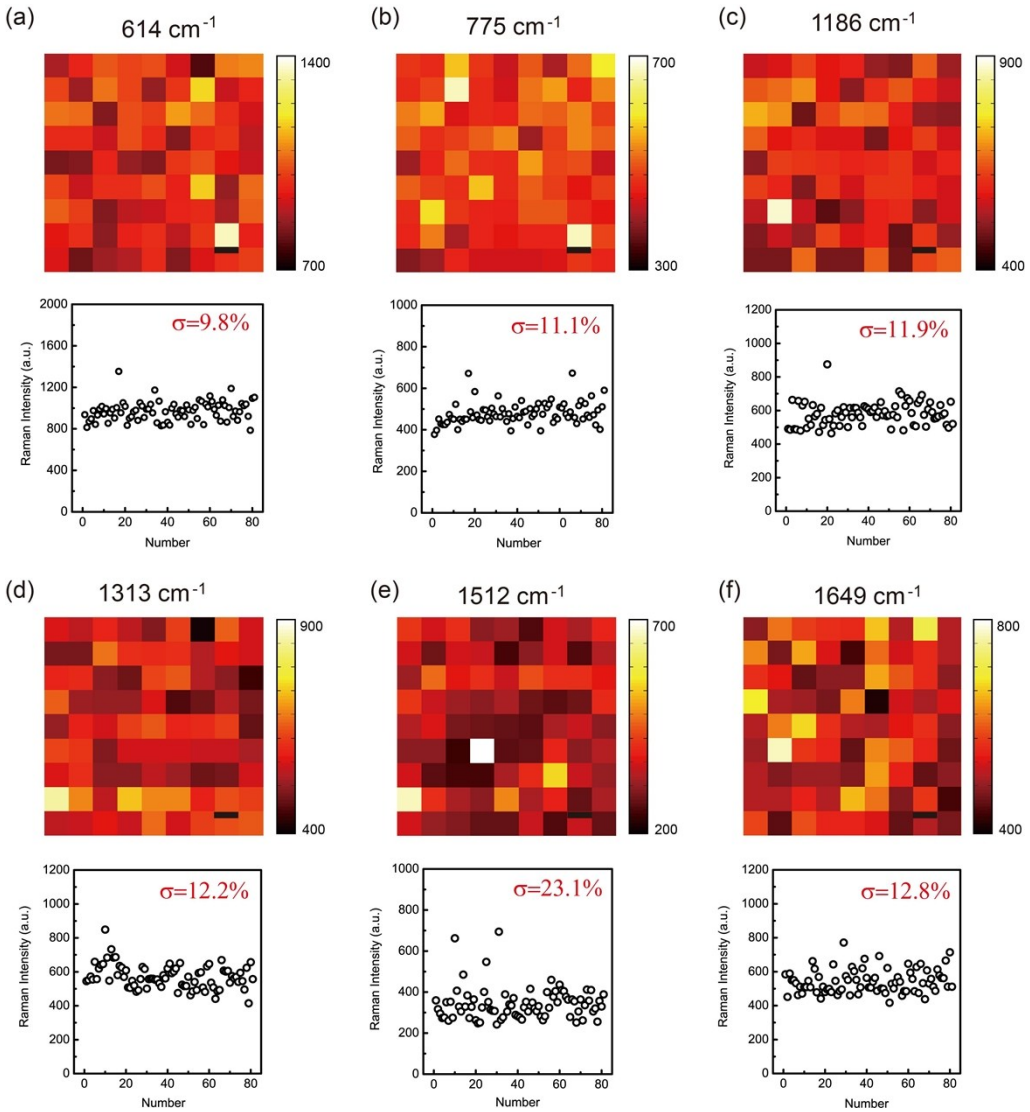

Fig. S6. Intensity mapping and distributions of SERS signal of R6G molecules adsorbed on a

GIGN (a = 400 nm, h = 150 nm) at other Raman bands. (a) 614 cm^{-1} (C-C-C bond stretching vibrations); (b) 775 cm^{-1}(the out-of-plane vibration of deformed C-H bonds); (c) 1186 cm^{-1}(the in-plane vibration of deformed C-H bonds); (d) 1313 cm^{-1}(C-C stretching modes); (e) 1512 cm^{-1}(C-C stretching modes); (f)1649 cm^{-1}(C-C stretching modes). The scanning step size is 10 μm. (a-f) Scale bars, 10 μm.

S11. Sample-to-sample reproducibility of GIGNs

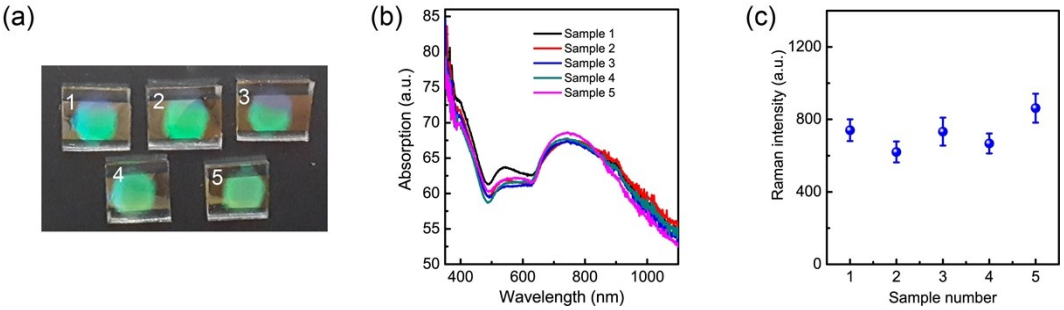

Fig.S7. Sample-to-sample reproducibility of GIGNs. (a) Optical photograph of the five GIGNs fabricated under the same conditions. (b) Absorption spectra of these five samples. (c) Raman intensity of R6G (10^{-6}mol/L) at 1361 cm^{-1} band for these five samples. Error bars indicate standard deviations of ten measurements for each sample. The sample-to-sample Raman intensity variation was determined to be 12.6%.

S12. Uniformity of SERS signal of MGITC molecules adsorbed on a GIGN

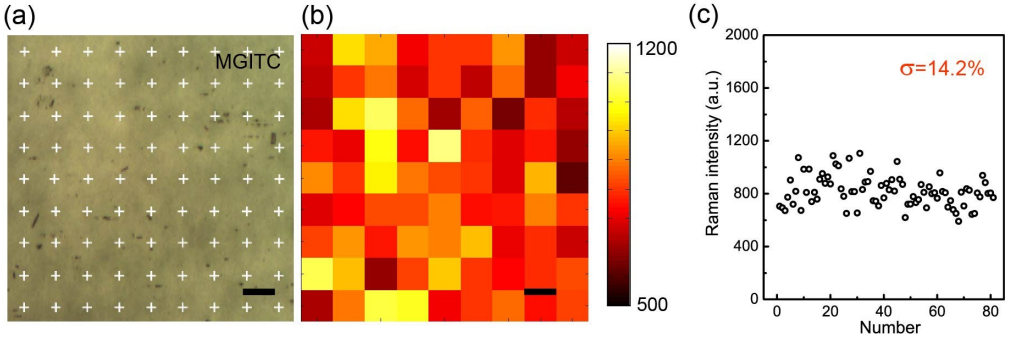

Fig. S8. Uniformity of SERS signals of MGITC molecules adsorbed on a GIGN. (a) Optical micrograph of a GIGN covered by MGITC molecules. (b) Intensity mapping of MGITC (10^{-7} M) for the area as shown in (a) at 1180 cm^{-1} band. (c) SERS intensity distribution of MGITC in mapping. The relative standard deviation is 14.2%. The sizes of the GIGN are a = 400 nm, h = 150 nm, w_1 = 220 nm, w_2 = 280 nm, l = 120 nm, d = 25 nm, θ = 15°, s_x = 37 nm and s_y = 80 nm. (a,b) Scale bars, 10 μm.